

Synthesis, Characterization, Molecular Modeling, Antimicrobial and DNA Binding Studies of Cobalt(II) Complexes of 2,3-(Diimino-4'-antipyrynyl)butane with Varying Counter Ions

B.N. ANILA^{1,*}, M.K. MURALEEDHARAN NAIR², JISHA SREEDHARAN³ and V.P. SYLAS⁴

¹Department of Chemistry, Government College Kottayam, Kottayam-686 013, India

²Department of Chemistry, Maharajas College, Ernakulam-682 011, India

³School of Chemical Sciences, Mahatma Gandhi University, Kottayam-686 560, India

⁴School of Environmental Sciences, Mahatma Gandhi University, Kottayam-686 560, India

*Corresponding author: E-mail: bnanila@gmail.com

Received: 12 October 2016;

Accepted: 8 December 2016;

Published online: 30 December 2016;

AJC-18228

The synthesis and characterization of perchlorate, nitrate, chloride, bromide and iodide complexes of cobalt(II) with a new Schiff base ligand 2,3-(diimino-4'-antipyrynyl)butane prepared from 4-aminoantipyryne and 2,3-butanedione have been done by elemental analysis, electrical conductance in non-aqueous solvents, infrared and electronic and ¹H NMR spectra as well as thermogravimetry. The UV-visible, magnetic susceptibility and ESR spectral data suggest an octahedral geometry around the central metal ion in chloro and bromo complexes and a tetrahedral geometry around the central metal ion for perchlorate, nitrate and iodide complexes. The molecular modeling of the proposed structure is in agreement with the above mentioned structure. Biological screening analyses of the ligands and the cobalt(II) complexes reveals that the Schiff base and its cobalt(II) complexes show significant activity against microorganisms. Binding studies of Co(II) complexes with calf thymus DNA (CT DNA) were studied by spectral methods such as absorption spectroscopy through the ethidium bromide (EB) displacement technique and viscosity measurements. The results obtained indicate that the complexes bind to DNA *via* intercalation.

Keywords: 2,3-(Diimino-4'-antipyrynyl)butane, Antipyryne, Cobalt(II) complexes, Antimicrobial studies, DNA binding studies.

INTRODUCTION

4-Aminoantipyryne and its versatile Schiff base derivatives have been extensively investigated and effectively applied in biological, analytical, clinical and pharmacological areas [1-4]. Antipyryne derivatives are reported to exhibit analgesic and anti-inflammatory effects [5,6], antiviral [7] and antibacterial [8] activities. It is also been used as hair colour additives [9] and to potentiate the local anesthetic effect of lidocaine [10]. These compounds have been used in spectrophotometric determination of metal ions. Many of these reagents give intense colours with transition metal ions, providing sensitive probes [11] and some of them can also coordinate to rare earth ions to form metal complexes with interesting structures [12]. The complexes derived from such ligands possess these physiological properties with varying intensity. Also most of these complexes are showing antitumor activities [13]. In the present investigation we have synthesized five complexes of cobalt(II) with varying counter ions with the Schiff base ligand 2,3-(diimino-4'-antipyrynyl)butane (BDAP). All the complexes were characterized with different analytical and spectrometric techniques and the structures of the complexes were confirmed

by molecular modeling. The application studies of these compounds such as the antimicrobial and DNA binding studies were also carried out.

EXPERIMENTAL

Five metal salts were used for the synthesis of complexes. Among them CoCl₂·6H₂O and Co(NO₃)₂·6H₂O were AR grade and Co(ClO₄)₂·6H₂O, CoBr₂·6H₂O CoI₂·6H₂O were prepared from Co(CO₃)₂ by treatment with corresponding 60 % acid. The ligand was prepared from 4-aminoantipyryne and 2,3-butanedione. The 4-aminoantipyryne and 2,3-butanedione were supplied by Sigma Aldrich Chemical Co. USA. These chemicals were used without further purification. For DNA binding studies Tris HCl, ethidium bromide and NaCl were A.R. grade and calf-thymus DNA was from Sigma Aldrich Chemical Co. USA. These chemicals were used without further purification. The solvents used were further purified by distillation.

Analyses of complexes: Cobalt present in the complexes was estimated by EDTA titration [14]. Chloride content was estimated by Volhard's method [14] and perchlorate content by Kurz's method [15]. The elemental analyses of the complexes were done using a Heraeus-CHN-Rapid analyzer. Molar

conductance of 10^{-3} M solutions of the complexes was measured using a Systronics conductivity bridge with a dip conductance cell having two platinum electrodes. The infrared spectra were recorded in a Shimadzu FTIR 8400 S spectrophotometer in the range $4000\text{--}400\text{ cm}^{-1}$ using KBr pellet technique and in a Bruker IFS 66v FTIR spectrometer in the range $500\text{--}100\text{ cm}^{-1}$ using polyethylene powder. Electronic spectral studies of the Schiff base and the complexes in solid state were carried out on a Shimadzu UV-visible spectrometer UV-2450 in the range $190\text{--}1100\text{ nm}$. Magnetic susceptibility measurements were done in a Sherwood Scientific Magnetic Susceptibility balance at room temperature. The molecular modeling of the complexes was done in Chem. 3D Ultra 15.1.0.144 version software using MM2 method for minimizing the energy.

Synthesis of ligand: The Schiff base, 2,3-(diimino-4'-antipyrynyl)butane was prepared by the condensation between 2,3-butanedione and 4-aminoantipyryne in ethyl acetate medium for about 5 h in 1:2 molar ratio. The yellow precipitate thus obtained was filtered and washed with hot ethyl acetate to remove the excess reactants. It was then recrystallized from ethanol and dried over phosphorous(V) oxide under vacuum. The yield was about 65 %. The scheme of synthesis is represented in Fig. 1.

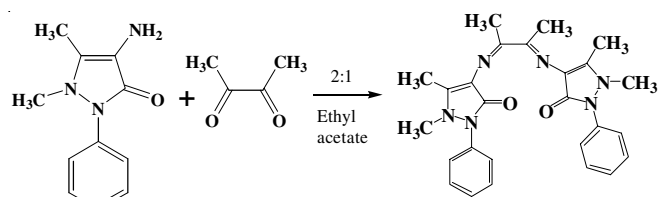


Fig. 1. Synthesis of 2,3-(diimino-4'-antipyrynyl)butane (BDAP)

The purity of ligand was checked by TLC, infrared, mass and NMR spectra and by elemental analysis. The melting point of the compound was found to be $245\text{ }^{\circ}\text{C}$. The molecular formula and molecular weight of the ligand were $\text{C}_{26}\text{H}_{28}\text{N}_6\text{O}_2$ and 456.44, respectively. The elemental analysis data is C = 68.38 (68.41), H = 5.34 (6.18) N = 18.11 (18.40).

Preparation of cobalt(II) complexes: A quantity of 1 mmol of $\text{Co}(\text{ClO}_4)_2 \cdot 6\text{H}_2\text{O}$, $\text{Co}(\text{NO}_3)_2 \cdot 6\text{H}_2\text{O}$, $\text{CoCl}_2 \cdot 6\text{H}_2\text{O}$, or $\text{CoBr}_2 \cdot 6\text{H}_2\text{O}$, in methanol (10 mL) or $\text{CoI}_2 \cdot 6\text{H}_2\text{O}$ in isopropyl alcohol (10 mL) were added to a boiling suspension of 1.2 mmol of BDAP in ethyl acetate (100 mL). The mixture was refluxed for about 5 h. The precipitated complexes were filtered and washed repeatedly with hot ethyl acetate to remove the excess ligand. These were then recrystallized from ethanol and dried under vacuum over phosphorous(V) oxide. The scheme of preparation of cobalt(II) complexes is represented in Fig. 2.

Molecular modeling: The 3D molecular modeling of the proposed structure of the ligand BDAP and its cobalt(II) complexes were performed by using Chem. 3D Ultra 15.1.0.144 version software using MM2 for minimizing energy. Molecular modeling usually gives a better insight on the molecular structure, geometric optimization and conformational analysis of the ligand and its complexes. The correct stereochemistry was assured through the modification and exploitation of the molecular coordinates to attain reasonable low energy mole-

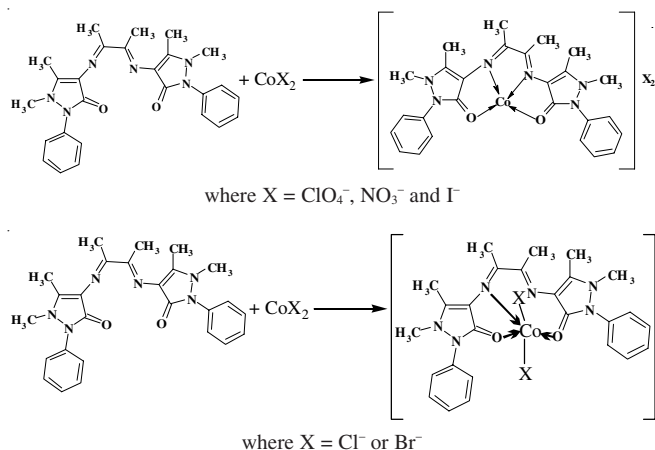


Fig. 2. Preparation of cobalt(II) complexes with varying counter ions

cular geometries. The potential energy of the molecule was considered as the sum of the following stipulations:

$$E = \text{Estr} + \text{Eang} + \text{Etor} + \text{Evdw} + \text{Eoop} + \text{Eele} \quad (3)$$

where E represents the energy values corresponding to the given type of interaction (kcal/mol). The subscripts str, ang, tor, vdw, oop and ele signify bond stretching, angle bonding, torsion deformation, van der Waals interactions, out of plane bending and electronic interaction, respectively.

Antimicrobial studies: The *in vitro* antimicrobial screening of the cobalt(II) complexes were tested for their effect on certain human pathogenic bacteria and fungus by well diffusion method [16,17]. 10^{-3} M solutions of all the complexes were prepared in DMF. Both the Gram-positive (*Escherichia coli* and *Bacillus subtilis*) and Gram-negative (*Vibrio parahaemolyticus*, *Salmonella typhi*, *Salmonella weltevreden*, *Aeromonas hydrophila*) bacteria were grown in nutrient agar medium and incubated at $37\text{ }^{\circ}\text{C}$ for 48 h followed by frequent subculture to Muller Hinton agar medium and were used as test bacteria. The fungi, *Trichophyton tonsurans* grown into the Sabouraud dextrose agar medium, incubated at $27\text{ }^{\circ}\text{C}$ for 72 h followed by periodic sub culturing to fresh medium and were used as test fungus. Then the Petri dishes were inoculated with a loop full of bacterial or fungal culture and spread throughout the Petri dishes uniformly with a sterile glass spreader. The test samples (10 mg/mL) and reference streptomycin (1 mg/mL for bacteria) or chlorothalonil (10 mg/mL for fungus) were added with a sterile micropipette in the wells of each plate. The plates were then incubated at $35 \pm 2\text{ }^{\circ}\text{C}$ and $27 \pm 1\text{ }^{\circ}\text{C}$ for 24-48 h for bacteria and fungus, respectively. Plates with well containing respective solvents served as control. Inhibition was recorded by measuring the diameter of the inhibitory zone after the period of incubation. All the experiments were repeated twice and average values are presented here.

DNA binding experiments

Preparation of tris-hydrochloride buffer: Tris-hydrochloride (197 mg, 5 mm) and sodium chloride (730 mg, 50 mm) were accurately weighed and made up to 250 mL using double distilled water. The pH of this solution was adjusted to 7.2 using 1 mm sodium hydroxide solution with the help of pH meter before making up to the mark. This buffer pH 7.2 was used for all DNA binding studies.

Absorption spectral studies: The UV-visible absorption spectroscopy studies and the DNA binding experiments were performed at room temperature. The purity of the CT-DNA was verified by taking the ratio of the absorbance values at 260 and 280 nm in Tris HCl buffer, which was found to be approximately 1.8 indicating that the DNA was sufficiently free of protein [18]. The DNA concentration per nucleotide was determined by absorption spectroscopy using the molar extinction coefficient value of $6600 \text{ dm}^3 \text{ mol}^{-1} \text{ cm}^{-1}$ at 260 nm [19]. The complexes were dissolved in methanol for all the experiments. Absorption spectra were recorded with a fixed concentration of the compounds (25 μM) while gradually increasing the concentration of DNA (10-50 μM). While measuring the absorption spectra, an equal amount of DNA was added to both the test solution and the reference solution to eliminate the absorbance of DNA itself. Further support for the complexes binding to DNA *via* intercalation is given through emission quenching experiments. DNA was pretreated with ethidium bromide for 30 min. Then the test solutions were added to this mixture of EB-DNA and the change in the fluorescence intensity was measured. The excitation and the emission wavelength were 515 and 603-607 nm, respectively.

Viscosity measurements: Viscosity experiments were carried out using a Schott Gerate AVS 310 automated viscometer that was thermostated at 25 °C in a constant temperature bath. The lengthening of the DNA helix has been examined in the absence and presence of increasing amounts of complexes. Flow time was measured with a digital stopwatch and for each sample the measurement was made in triplicates and the mean value of flow time was recorded [20]. The obtained data are presented as $(\eta/\eta^0)^{1/3}$ versus the binding ratio, where η is the viscosity of CT-DNA in the presence of complex and η^0 is the viscosity of CT-DNA alone in buffer solution.

RESULTS AND DISCUSSION

The cobalt(II) complexes are light brown, non-hygroscopic solids which are soluble in acetonitrile, benzene, DMF, DMSO, ethanol and methanol and are insoluble in acetone, ethyl acetate and nitrobenzene.

The metal, bromide, chloride, perchlorate, carbon, nitrogen and hydrogen content in the cobalt(II) complexes were determined and presented in Table-1. The data suggests that the complexes may be formulated as $\text{Co}(\text{BDAP})\text{X}_2$ ($\text{X} = \text{ClO}_4^-$, NO_3^- , Cl^- , Br^- or I^-).

Electrical conductance: The molar conductance values of the cobalt(II) complexes of BDAP (10^{-3} M solution) were measured in acetonitrile, DMF, ethanol and methanol and the values are given in Table-2. The molar conductance values of the complexes fall in the range suggests 1:2 electrolytes for perchlorate, nitrate and iodide complexes and non-electrolyte for chloride and bromide complexes [21]. Thus the complexes may be formulated as $[\text{Co}(\text{BDAP})]\text{X}_2$ ($\text{X} = \text{ClO}_4^-$, NO_3^- or I^-) and $\text{Co}(\text{BDAP})\text{X}_2$ ($\text{X} = \text{Cl}^-$ or Br^-).

Infrared spectra: The important infrared spectral bands of BDAP and its cobalt(II) complexes together with the tentative assignments are given in Table-3.

The infrared spectrum of the ligand BDAP shows strong bands at 1649 and 1593 cm^{-1} , characteristic of both carbonyl [22] and azomethine [23,24] groups, respectively. The strong infrared band observed at 1649 cm^{-1} , characteristic of C=O stretching vibration of BDAP is found to be shifted to the region $1618\text{-}1612 \text{ cm}^{-1}$ in all the complexes showing that both the carbonyl oxygens are coordinated in these complexes [25]. Also the intense band due to C=N stretching vibration is shifted to the region $1581\text{-}1562 \text{ cm}^{-1}$ in all the complexes indicating the coordination of both the azomethine nitrogens [26]. From the infrared spectral data, it is concluded that the Schiff base BDAP acts as a neutral tetradentate ligand, coordinating through both the carbonyl oxygens and both the azomethine nitrogens resulting in the formation of three five membered rings, there by imparting considerable stability to the complexes.

In the perchlorate complex, an intense un-split band observed at 1080 cm^{-1} is assigned to the ν_3 vibration of uncoordinated perchlorate ion of T_d symmetry [27]. The ν_4 vibration of the perchlorate (T_d) ion is observed at 624 cm^{-1} , also support the existence of uncoordinated perchlorate ion in the complex [27].

In the nitrate complex, a very strong band observed at 1382 cm^{-1} indicates the presence of uncoordinated nitrate ion

TABLE-1
ANALYTICAL DATA OF COBALT(II) COMPLEXES OF BDAP

Complex	m.f.	m.w.	m.p. (°C)	Elemental analysis (%): Found (Calcd.)				
				Metal	Anions	Carbon	Hydrogen	Nitrogen
$[\text{Co}(\text{BDAP})](\text{ClO}_4)_2$	$\text{C}_{26}\text{H}_{28}\text{N}_6\text{O}_8\text{CoCl}_2$	714.38	162	8.19 (8.24)	27.65 (27.84)	43.63 (43.71)	3.97 (3.9)	11.81 (11.76)
$[\text{Co}(\text{BDAP})](\text{NO}_3)_2$	$\text{C}_{26}\text{H}_{28}\text{N}_8\text{O}_6\text{Co}$	639.48	159	9.34 (9.21)	–	48.18 (48.83)	4.32 (4.41)	18.02 (17.52)
$[\text{Co}(\text{BDAP})\text{Cl}_2]$	$\text{C}_{26}\text{H}_{28}\text{N}_6\text{CoCl}_2$	586.38	167	10.01 (10.05)	11.95 (12.09)	52.95 (5.25)	5.08 (4.81)	14.28 (14.33)
$[\text{Co}(\text{BDAP})\text{Br}_2]$	$\text{C}_{26}\text{H}_{28}\text{N}_6\text{CoBr}_2$	676.18	196	8.66 (8.71)	23.75 (23.63)	45.85 (46.18)	4.39 (4.17)	12.39 (12.42)
$[\text{Co}(\text{BDAP})\text{I}_2]$	$\text{C}_{26}\text{H}_{28}\text{N}_6\text{CoI}_2\text{Cl}_2$	761.10	170	7.69 (7.66)	33.05 (32.9)	40.32 (40.56)	3.84 (3.64)	10.90 (10.92)

TABLE-2
MOLAR CONDUCTANCE ($\text{ohm}^{-1} \text{ cm}^2 \text{ mol}^{-1}$) DATA OF COBALT(II) COMPLEXES (10^{-3} M SOLUTION) OF BDAP

Complex	Molar conductance				
	Acetonitrile	DMF	Methanol	Ethanol	Type of electrolyte
$[\text{Co}(\text{BDAP})](\text{ClO}_4)_2$	282.1	163.8	199.6	90.5	1:2
$[\text{Co}(\text{BDAP})](\text{NO}_3)_2$	223.5	147.5	201.81	82.4	1:2
$[\text{Co}(\text{BDAP})\text{Cl}_2]$	112.8	57.47	–	25.45	non-electrolyte
$[\text{Co}(\text{BDAP})\text{Br}_2]$	100.3	–	46.24	–	non-electrolyte
$[\text{Co}(\text{BDAP})\text{I}_2]$	185.1	145.2	203.03	75.6	1:2

TABLE-3
KEY INFRARED SPECTRAL BANDS (cm⁻¹) OF BDAP AND ITS COBALT(II) COMPLEXES

BDAP	[Co(BDAP)](ClO ₄) ₂	[Co(BDAP)](NO ₃) ₂	[Co(BDAP)]Cl ₂	[Co(BDAP)]Br ₂	[Co(BDAP)]I ₂	Assignments
1649	1612	1618	1612	1618	1614	v(C=O)
1593	1581	1571	1562	1571	1566	v(C=N)
	1091					v ₃ uncoordinated ClO ₄
	624					v ₄ uncoordinated ClO ₄
		1384				v ₃ uncoordinated NO ₃
		827				v ₂ uncoordinated NO ₃
	280		280			v(Co-Cl)
				280		v(Co-Br)
	554	553	554	554	552	v(Co-O)
	453	453	453	452	453	v(Co-N)

in this complex which is due to v₃ vibration of the nitrate ion of D_{3h} symmetry [28]. This is supported by another medium intensity band observed at 825 cm⁻¹ which is attributed to the v₂ vibration of the uncoordinated nitrate ion of D_{3h} symmetry. In the far IR spectrum of the chloro and bromo complexes the v(Co-Br) and v(Co-Cl) and bands observed at 280 cm⁻¹, respectively which are not present in the spectrum of the ligand. The above IR spectral results are in conformity with the conductance data that both the perchlorate, both the nitrate and both the iodides remain as counter and both the chloride and both the bromide ions are coordinated to the metal ion in all the complexes. Further the v(Co-O) and v(Co-N) stretching vibrations are observed at about 554 and 453 cm⁻¹, respectively in all the complexes [29].

¹H NMR spectra: The proton NMR spectral data of the BDAP and its Co(II) complexes were presented in Table-4. BDAP shows a singlet at δ 2.84 which is assigned to the -N=C-CH₃ protons and a multiplet in the region δ 7.22-7.37 due to phenyl protons [30]. In all the complexes the multiplet due to phenyl protons is shifted to the region δ 7.45-7.46. This indicates the coordination of carbonyl oxygen to the metal. The singlet at δ 2.8 due to -N=C-CH₃ protons in BDAP is shifted to the region δ 2.90-3.08 in the complexes showing the coordination of azomethine nitrogen.

Electronic spectral studies: The electronic spectral studies of cobalt(II) complexes of BDAP with tentative assignments are listed in Table-5. The electronic spectra of the ligand BDAP shows two absorption maxima at 26810 and 42735 cm⁻¹ corresponding to n→π* and π→π* transitions, respectively [31]. But in cobalt(II) complexes, both n→π* and π→π* transitions are found to be red shifted to the regions 25126-26667 cm⁻¹ and 37593-39370 cm⁻¹, respectively when compared to that of BDAP [32]. Also an intense absorption band observed in the region 30674-31446 cm⁻¹ in all the complexes may be due to charge transfer transitions. The absorption bands observed

in the region 21739-21834 cm⁻¹, 15038-15948 cm⁻¹ and 8976-9009 cm⁻¹ of the chloro and bromo complexes of cobalt(II) may be assigned to ⁴T_{1g}(F)→⁴T_{1g}(P), ⁴T_{1g}(F)→⁴A_{2g}(F) and ⁴T_{1g}(F)→⁴T_{2g}(F) transitions, respectively, which are in agreement with a high spin octahedral geometry of the complexes around cobalt(II) ion [33,34]. Furthermore in the electronic spectra of the perchlorate, nitrate and iodide complexes of cobalt(II), three closely spaced weak bands were observed in the region 16946-17241 cm⁻¹, 14368-16025 cm⁻¹ and 13850-15060 cm⁻¹ which are assigned to be ⁴A₂(F)→⁴T₁(P) transition for a distorted tetrahedral symmetry around the cobalt(II) ion [32]. The splitting of the spectral lines originates from the restricted bond angle of the O-Co-N entity [35,36].

Magnetic behaviour: The magnetic susceptibility measurements of all the cobalt(II) complexes were done and the magnetic moment values are presented in Table-5 along with electronic spectral data. The magnetic moment values are in the range 4.23-4.4 BM suggesting tetrahedral configuration around the cobalt(II) ion in perchlorate, nitrate and iodide complexes [37] while the value in the range of 4.76-4.84 BM suggesting a octahedral configuration around the cobalt(II) ion in chloride and bromide complexes [34]. The observed values for tetrahedral configuration are higher than the spin only value (3.87 BM). This may be due to the incomplete quenching of orbital moment by the surrounding ligands [34].

Thermogravimetric analyses: The thermogravimetric analysis of cobalt(II) complexes of BDAP were done and the phenomenological kinetic as well as mechanistic aspect of thermal decomposition is discussed here. The data of the thermal analysis are presented in Tables 6-8.

Thermal analysis reveals that, the complexes are stable up to a temperature range 173-230 °C. All the complexes undergo a two stage decomposition pattern. The iodide complex is the least stable and the bromo complex is the most stable. The thermal stability of the complexes is in the order bromo > chloro

TABLE-4
IMPORTANT ¹H NMR PEAKS OF BDAP AND ITS Co(II) COMPLEXES (IN δ w.r.t. TMS)

Complex	-CH ₃	=C-CH ₃	-N-CH ₃	Phenyl multiplet
BDAP	2.15 (sh,s)	2.84 (sh,s)	3.18 (sh,s)	7.22-7.37 (br,m)
[Co(BDAP)](ClO ₄) ₂	2.32	2.90	3.21	7.45-7.46
[Co(BDAP)](NO ₃) ₂	2.18	2.91	3.23	7.44-7.46
[Co(BDAP)]Cl ₂	2.22	2.91	3.19	7.45-7.46
[Co(BDAP)]Br ₂	2.28	3.08	3.21	7.45-7.46
[Co(BDAP)]I ₂	2.23	2.92	3.22	7.44-7.46

sh = sharp; s = strong; br = broad; m = multiplet

TABLE-5
ELECTRONIC SPECTRAL DATA AND MAGNETIC MOMENT VALUES OF COBALT(II) COMPLEXES OF BDAP

Complex	Absorbance max. (cm ⁻¹)	Tentative assignments	μ_{eff} (BM)
[Co(BDAP)](ClO ₄) ₂	25,126	n→π*	4.32
	38,314	π→π*	
	30864	Charge Transfer	
	17241	⁴ A ₂ (F) → ⁴ T ₁ (P)	
	16025	⁴ A ₂ (F) → ⁴ T ₁ (P)	
[Co(BDAP)](NO ₃) ₂	25316	n→π*	4.40
	37,593	π→π*	
	31152	Charge Transfer	
	16946	⁴ A ₂ (F) → ⁴ T ₁ (P)	
	16025	⁴ A ₂ (F) → ⁴ T ₁ (P)	
[Co(BDAP)Cl ₂]	25,974	n→π*	4.84
	38,168	π→π*	
	31446	Charge Transfer	
	21739	⁴ T _{1g} (F) → ⁴ T _{1g} (P)	
	15,948	⁴ T _{1g} (F) → ⁴ A _{2g} (F)	
[Co(BDAP)Br ₂]	26,667	n→π*	4.76
	38,168	π→π*	
	31055	Charge Transfer	
	21834	⁴ T _{1g} (F) → ⁴ T _{1g} (P)	
	15038	⁴ T _{1g} (F) → ⁴ A _{2g} (P)	
[Co(BDAP)]I ₂	25,849	n→π*	4.23
	39,370	π→π*	
	30674	Charge Transfer	
	16949	⁴ A ₂ (F) → ⁴ T ₁ (P)	
	14,368	⁴ A ₂ (F) → ⁴ T ₁ (P)	
	13850	⁴ A ₂ (F) → ⁴ T ₁ (P)	

TABLE-6
PHENOMENOLOGICAL DATA FOR THE THERMAL DECOMPOSITION OF THE COBALT(II) COMPLEXES OF BDAP

Complexes	Stages of decomposition	Temp. (K)	DTA peak (°C)	Residual species	Decomposition species	Total mass loss (%)	
						Found	Calcd.
[Co(BDAP)](ClO ₄) ₂	I	193-316	272	CoO	Two perchlorate ions	27.69	27.84
	II	316-556	478		One molecule BDAP	62.83	63.89
[Co(BDAP)](NO ₃) ₂	I	183-286	250	CoO	Two nitrate ions	19.12	19.39
	II	286-530	410		One molecule BDAP	71.29	71.37
[Co(BDAP)Cl ₂]	I	211-370	295	CoO	Two chloride ions	11.54	12.09
	II	370-619	558		One molecule BDAP	77.8	77.84
[Co(BDAP)Br ₂]	I	219-419	302	CoO	Two bromide ions	24.24	23.63
	II	419-711	628		One molecule BDAP	66.15	67.5
[Co(BDAP)]I ₂	I	173-377	356	CoO	Two iodide ions	33.05	33.34
	II	377-476	434		One molecule BDAP	59.21	59.97

TABLE-7
KINETIC PARAMETERS FOR THE THERMAL DECOMPOSITION OF THE COBALT(II) COMPLEXES OF BDAP

Complex	Stages of decomposition	E (KJ mol ⁻¹)	A (s ⁻¹)	ΔS (JK ⁻¹ mol ⁻¹)
[Co(BDAP)](ClO ₄) ₂	I	97.46	2.17	-245.43
	II	80.29	1.091	-251.86
[Co(BDAP)](NO ₃) ₂	I	84.59	36.95	-219.56
	II	61.57	0.3609	-260.26
[Co(BDAP)Cl ₂]	I	64.97	1.2126	-248.66
	II	61.69	0.1726	-268.62
[Co(BDAP)Br ₂]	I	58.37	0.7342	-252.93
	II	100.67	2.155	-247.71
[Co(BDAP)]I ₂	I	31.24	3.62(E-02)	-278.88
	II	158.36	841.55	-196.29

> perchlorate > nitrate > iodide. The complexes are formulated as [Co(BDAP)]X₂ where X= ClO₄⁻, NO₃⁻ or I⁻ and [Co(BDAP)X₂] where X= Cl⁻ or Br⁻.

In perchlorate complex there is no mass loss up to 193 °C indicating the absence of water or any solvent molecules. The first stage starts at 193 °C and ends at 316 °C. The corresponding mass loss (27.69 %) is due to the decomposition of two perchlorate ions. The maximum rate of mass loss occurs at 272 °C as indicated by DTG peak. The second stage starts at 316 °C and ends at 556 °C with a DTG peak at 478 °C. The corresponding mass loss (62.83 %) is due to the decomposition of the BDAP molecule. The decomposition gets completed at 560 °C and the final residue is qualitatively proved to be anhydrous CoO.

TABLE-8
CORRELATION COEFFICIENTS CALCULATED USING THE NINE FORMS OF $g(\alpha)$ FOR COBALT(III) COMPLEXES OF BDAP

No.	Forms of $g(\alpha)$	Correlation coefficient (r)									
		Perchlorate complex		Nitrate complex		Chloride complex		Bromide complex		Iodide complex	
		Stage I	Stage II	Stage I	Stage II	Stage I	Stage II	Stage I	Stage II	Stage I	Stage II
1	α^2	-0.9863	-0.9543	-0.9448	-0.9889	-0.9671	-0.9612	-0.9735	-0.9616	-0.9819	-0.9516
2	$\alpha+(1-\alpha) \ln (1-\alpha)$	-0.9872	-0.9664	-0.9683	-0.9922	-0.9845	-0.9723	-0.9806	-0.9669	-0.9889	-0.9594
3	$[1-(1-\alpha)^{1/3}]^2$	-0.9752	-0.9294	-0.9137	-0.9817	-0.9457	-0.9217	-0.9583	-0.9472	-0.9510	-0.9423
4	$[(1-2/3\alpha)]-1-\alpha)^{2/3}$	-0.9873	-0.9709	-0.9783	-0.9933	-0.9939	-0.9763	-0.9831	-0.9688	-0.9912	-0.9622
5	$-\ln(1-\alpha)$	-0.9856	-0.9850	-0.9927	-0.9957	-0.9711	-0.9870	-0.9905	-0.9735	-0.9963	-0.9723
6	$[-\ln(1-\alpha)]^{1/2}$	-0.9754	-0.9779	-0.9910	-0.9932	-0.9652	-0.9775	-0.9859	-0.9641	-0.9907	-0.9674
7	$[-\ln(1-\alpha)]^{1/3}$	-0.9537	-0.9657	-0.9885	-0.9876	-0.9571	-0.9548	-0.9776	-0.9497	-0.9671	-0.9616
8	$1-(1-\alpha)^{1/2}$	-0.9838	-0.9677	-0.9802	-0.9921	-0.9930	-0.9713	-0.9811	-0.9650	-0.9882	-0.9607
9	$1-(1-\alpha)^{1/3}$	-0.9846	-0.9743	-0.9892	-0.9936	-0.9947	-0.9775	-0.9847	-0.9680	-0.9918	-0.9647

In nitrate complex there is no mass loss up to 183 °C indicating the absence of water or any solvent molecules. The first stage starts at 183 °C and ends at 286 °C. The corresponding mass loss (19.12 %) is due to the decomposition of two nitrate ions. The maximum rate of mass loss occurs at 250 °C as indicated by DTG peak. The second stage starts at 286 °C and ends at 530 °C with a DTG peak at 410 °C. The corresponding mass loss (71.29 %) is due to the decomposition of the BDAP molecule. The decomposition gets completed at 530 °C and the final residue is qualitatively proved to be anhydrous CoO.

In chloro complex there is no mass loss up to 211 °C indicating the absence of water or any solvent molecules. The first stage starts at 211 °C and ends at 370 °C. The corresponding mass loss (11.54 %) is due to the decomposition of two chloride ions. The maximum rate of mass loss occurs at 295 °C as indicated by DTG peak. The second stage starts at 370 °C and ends at 619 °C with a DTG peak at 558 °C. The corresponding mass loss (77.8 %) is due to the decomposition of the BDAP molecule. The decomposition gets completed at 620 °C and the final residue is qualitatively proved to be anhydrous CoO.

In bromo complex there is no mass loss up to 219 °C indicating the absence of water or any solvent molecules. The first stage starts at 219 °C and ends at 419 °C. The corresponding mass loss (24.64 %) is due to the decomposition of two bromide ions. The maximum rate of mass loss occurs at 302 °C as indicated by DTG peak. The second stage starts at 419 °C and ends at 711 °C with a DTG peak at 628 °C. The corresponding mass loss (66.15 %) is due to the decomposition of the BDAP molecule. The decomposition gets completed at 712 °C and the final residue is qualitatively proved to be anhydrous CoO.

In iodide complex there is no mass loss up to 173 °C indicating the absence of water or any solvent molecules. The first stage starts at 173 °C and ends at 377 °C. The corresponding mass loss (33.05 %) is due to the decomposition of two iodide ions. The maximum rate of mass loss occurs at 356 °C as indicated by DTG peak. The second stage starts at 377 °C and ends at 476 °C with a DTG peak at 434 °C. The corresponding mass loss (59.21 %) is due to the decomposition of the BDAP molecule. The decomposition gets completed at 480 °C and the final residue is qualitatively proved to be anhydrous CoO.

Kinetic aspects: The activation energies (E) of all the complexes of different stages of thermal decomposition are in the range of 31.24-158.36 KJ mol⁻¹. The corresponding values of pre-exponential factor for these complexes vary in the range $3.62 \times 10^{-2} - 841.55 \text{ S}^{-1}$. The respective values of entropy of activation (ΔS) are in the range -196.29 to -278.88 J mol⁻¹. It is observed that the energy of activation and pre-exponential factor of the second stage of decomposition of all the complexes except bromide and iodide complexes are lower than that of the first stage [38]. But the entropy of activation of the second stage of decomposition of all the complexes except bromide and iodide complexes are higher than that of the first stage. The negative values of entropy of activation indicate that the activated complex has a more ordered structure than the reactant and the reactions are slower than the normal [39].

Mechanistic aspects: The highest values of the magnitude of correlation coefficient is obtained for the equation:

$$g(\alpha) = -\ln(1-\alpha)$$

for all the stages of decomposition of all the complexes except for the first stage of perchlorate and chloride complex. Hence the mechanism for the decomposition is random nucleation with one nucleus on each particle representing 'Mampel Model' [39].

For the first stage of perchlorate complex, the highest value of the magnitude of correlation coefficient is obtained for the equation:

$$g(\alpha) = [(1-2/3\alpha)]-1-\alpha)^{2/3}$$

Hence the mechanism is three dimensional diffusion spherical symmetry representing Ginstling- Brounshtien equation.

For the first stage of chloride complex, the highest value of the magnitude of correlation coefficient is obtained for the equation:

$$g(\alpha) = 1-(1-\alpha)^{1/3}$$

Hence the mechanism is phase boundary reaction representing spherical symmetry [38].

Molecular modeling: The analytical, spectral and magnetic studies of the perchlorate, complex of cobalt(II) shows a tetra coordination and chloro and bromo complexes of cobalt(II) shows a hexacoordination which were further confirmed by their molecular modeling studies. The 3D optimized geometrical structures of ligand BDAP and its cobalt(II) complexes with varying counter ions are presented in the Figs.

3-6. The minimum steric energy which was repeated several times to find out the global minimum obtained to be 85.119, 244.837, 62.112, 455.836 and 231.653 kcal/mol, respectively. The obtained bond lengths of the ligand BDAP were in between C(13)-O(22) 1.231 Å, C(32)-O(34) 1.209 Å, C(1)-N(3) 1.281 Å and C(2)-N(4) 1.277 Å.

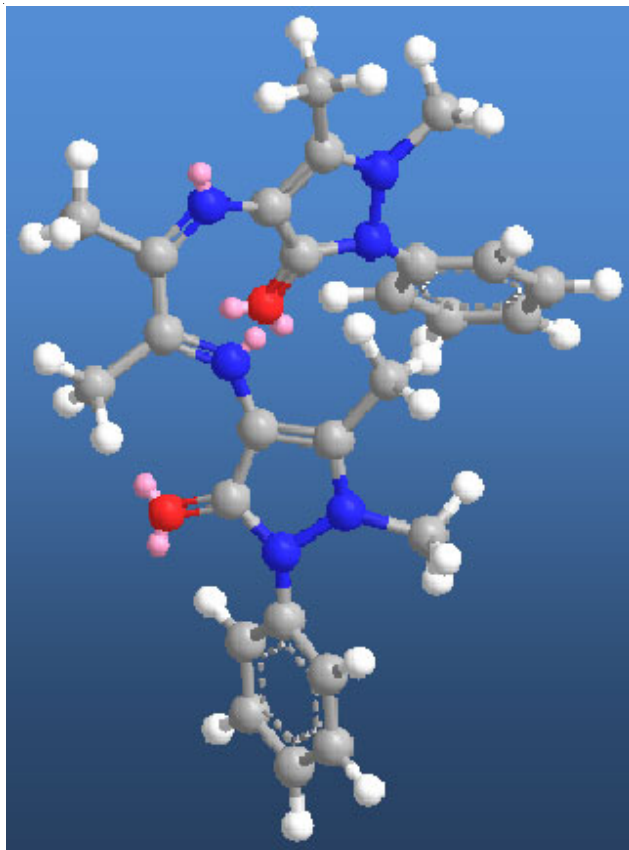


Fig. 3. Molecular modeling of the ligand BDAP

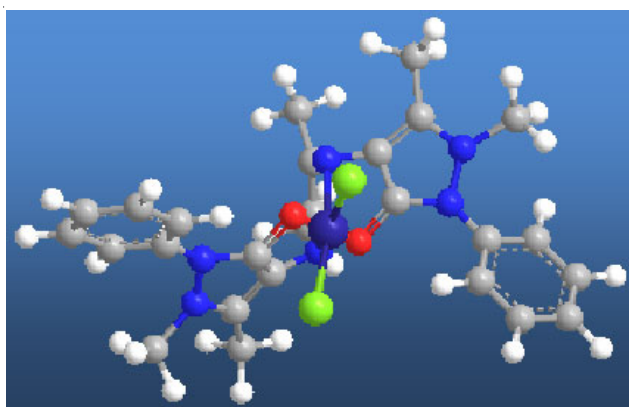


Fig. 4. Molecular modeling of [Co(BDAP)Cl₂]

Hence it was inferred that, when the ligand BDAP containing donor atoms such as carbonyl oxygens and azomethine nitrogens were coordinated with the metal ions by donating a lone pair of electrons results in decrease of electron density on the coordinating atoms, at the same time increase in the bond lengths and bond distance [40]. Furthermore in most of the cases, the actual bond angles and lengths are close to the optimal values thereby supporting the proposed tetra- and

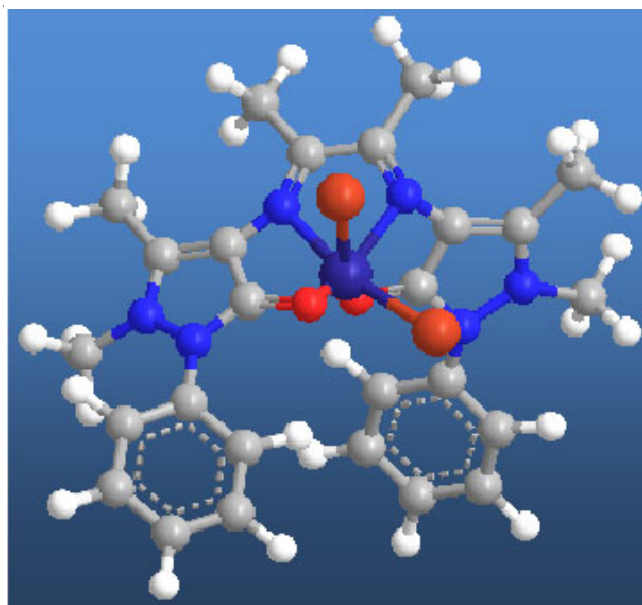


Fig. 5. Molecular modeling of [Co(BDAP)Br₂]

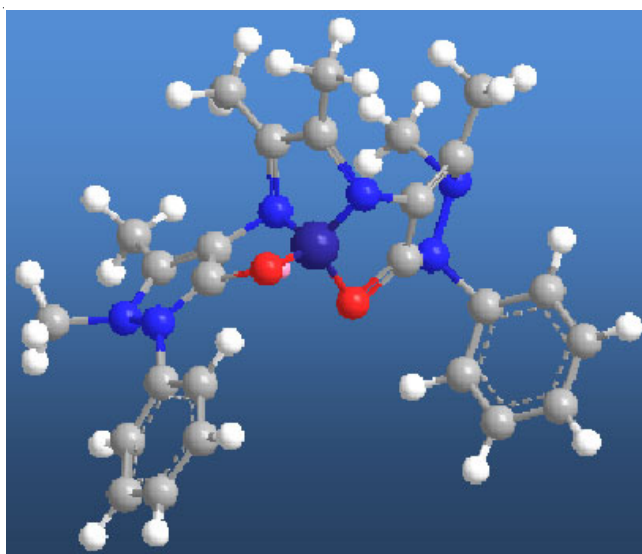


Fig. 6. Molecular modeling of [Co(BDAP)](ClO₄)₂

hexacoordinated geometry around the metal ion of these compounds [41]. The important bond lengths of cobalt(II)-chloride complex of BDAP is given in Table-9.

TABLE-9
IMPORTANT BOND LENGTHS OF COBALT(II)
CHLORIDE COMPLEX OF BDAP

Atom	Bond atom	Bond length (Å)
C(1)	N(3)	1.404
C(16)	N(3)	1.424
C(2)	N(4)	1.429
C(18)	N(4)	1.383
C(13)	O(22)	1.355
C(22)	O(34)	1.367
N(3)	Co(35)	1.876
N(4)	Co(35)	1.868
O(22)	Co(35)	1.837
O(34)	Co(35)	1.843
Br(36)	Co(35)	2.335
Br(37)	Co(35)	2.334

TABLE-10
ANTIBACTERIAL ACTIVITY OF BDAP AND ITS COBALT(II) COMPLEXES (ZONE DIAMETER IN mm)

Compound	<i>V. parahaemolyticus</i>	<i>S. typhi</i>	<i>A. hydrophila</i>	<i>B. subtilis</i>	<i>E. coli</i>	<i>S. weltevreden</i>
BDAP	0	20	23	0	19	19
[Co(BDAP)](ClO ₄) ₂	16	23	30	15	20	20
[Co(BDAP)](NO ₃) ₂	0	24	26	0	21	21
[Co(BDAP)]I ₂	0	25	25	0	20	21
[Co(BDAP)Cl ₂]	5	24	23	0	23	22
[Co(BDAP)Br ₂]	0	26	28	0	24	22
Standard (Streptomycin)	4	15	16	13	12	15

Antimicrobial analysis

Antibacterial screening: The antibacterial analysis results of Co(II) complexes are presented in Table-10. The Schiff base ligand BDAP and its cobalt(II) complexes were showing a very good antibacterial activity against all the four Gram-positive and Gram-negative bacteria among the six bacteria compared to the standard. Generally, the complexes have higher activity than the Schiff base ligand. A possible explanation for the observed increased activity upon chelation is that the positive charge of the metal in chelated complex is partially shared with the ligand's donor atoms so that there is an electron delocalization over the whole chelate ring. This in turn, will increase the lipophilic character of the metal [42]. BDAP and its cobalt(II) complexes are not showing any activity against two bacteria, *V. parahaemolyticus* and *B. subtilis*. Thus, the antibacterial activity of BDAP and its Co(II) complexes are [Co(BDAP)](ClO₄)₂ > [Co(BDAP)](NO₃)₂ > [Co(BDAP)]I₂ > [Co(BDAP)Cl₂] > [Co(BDAP)Br₂] > BDAP. All the complexes seem to be promising as they showed antibacterial activity higher than standard streptomycin.

Antifungal studies: The antifungal analysis results of Co(II) complexes are summarized in Table-11. All the complexes were showing a good antifungal activity against *Trichophyton tonsurans* compared to the standard. Generally, the metal complexes have higher activity than the Schiff base ligand. A possible explanation for the observed increased activity upon chelation is that the positive charge of the metal in chelated complex is partially shared with the ligand's donor atoms so that there is an electron delocalization over the whole chelate ring. This, in turn, will increase the lipophilic character of the metal [42]. It is concluded that antifungal activity of bromo and iodide complexes of Co(II) complexes is higher than other complexes.

DNA binding studies: The DNA binding analyses of the complexes were carried out by using electronic spectra, fluorescence spectra and viscosity measurements.

TABLE-11
ANTIFUNGAL ACTIVITY OF BDAP AND ITS
COBALT(II) COMPLEXES (ZONE DIAMETER IN mm)

Compound	<i>Trichophyton tonsurans</i>
BDAP	14
[Co(BDAP)](ClO ₄) ₂	16
[Co(BDAP)](NO ₃) ₂	16
[Co(BDAP)]I ₂	18
[Co(BDAP)Cl ₂]	16
[Co(BDAP)Br ₂]	19
Chlorothalonil	34
DMSO	0

Electronic spectral studies: Electronic absorption spectroscopy has been widely used to determine the binding ability of metal complexes with DNA. The binding ability of the synthesized Co(II) complexes [Co(BDAP)](ClO₄)₂ (**1**), [Co(BDAP)](NO₃)₂ (**2**), [Co(BDAP)Cl₂] (**3**), [Co(BDAP)Br₂] (**4**) and [Co(BDAP)I₂] (**5**) with CT-DNA were studied by measuring the spectral changes of their electronic spectra during the interaction with DNA. The complexes binding with DNA through intercalation usually results in bathochromism or hypochromism due to intercalative mode involving a strong stacking interaction between the base pairs of DNA [43] and an aromatic chromophore of the bound ligand. Therefore, in order to obtain the evidence for the binding mode of complexes with DNA, spectroscopic analyses of complex solutions with DNA have been performed. Absorption titration experiments of complexes in Tris-HCl buffer were performed by using a fixed concentration of complexes to which increments of the DNA stock solution were added. The absorption spectra of complexes **1-5** in the absence and presence of DNA are given in Figs. 7-11. The binding of complexes to DNA led to decrease in the absorption intensities (hypochromism) with a small amount of red shifts in the UV-visible absorption spectra (bathochromism). The extent of hypochromism depends on intercalative interaction [44]. After intercalating the base pairs of DNA, the π orbital of the base pairs can couple with the π^* orbital of the intercalated ligand, thus decreasing the π - π^* transition energy and resulting in the bathochromism [45]. To compare quantitatively the affinity of the complexes toward DNA, the binding constants k_b of the complexes **1** and **2** to CT-DNA were determined by monitoring the changes of absorbance at 261 and 260 nm for complexes **1** and **2**, respectively, with increasing concentration of DNA. The red shift of λ_{max} band and considerable decrease in absorption intensity suggest that the complexes bind to DNA strongly [46]. Using the absorption titration data, the binding constant (k_b) was determined from the following equation [47]:

$$\frac{c}{\Delta\epsilon_a} = \frac{c}{\Delta\epsilon} + \frac{1}{\Delta\epsilon k_b}$$

where $c = [DNA]$; $\Delta\epsilon_a = |\epsilon_a - \epsilon_f|$ and $\Delta\epsilon = |\epsilon_b - \epsilon_f|$ (ϵ_a , ϵ_f and ϵ_b are extinction coefficient of the observed ($A_{obs}/[complex]$), the free complex and the complex fully bound to DNA, respectively). The ratio of slope to intercept in the plot of $[DNA]/\Delta\epsilon_a$ vs. $[DNA]$ gave the value of K_b . The binding constants (K_b) of complexes **1** and **2** are calculated as 2.68×10^6 and 1.12×10^6 M⁻¹, respectively. The obtained K_b values are in agreement with those of DNA-intercalative Schiff base cobalt(II) complexes [48] and revealed that the perchlorate complex is moderate

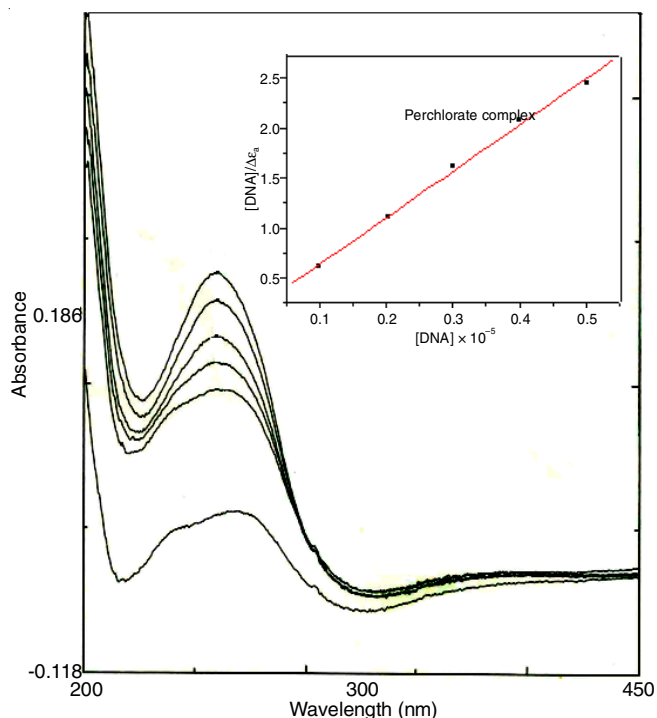


Fig. 7. Absorption spectra of the perchlorate complex of BDAP in Tris-HCl buffer upon addition of different concentrations of CT-DNA. Plot for $[DNA]/\Delta\epsilon_a$ vs. $[DNA]$ for absorption titration of CT-DNA with the complex

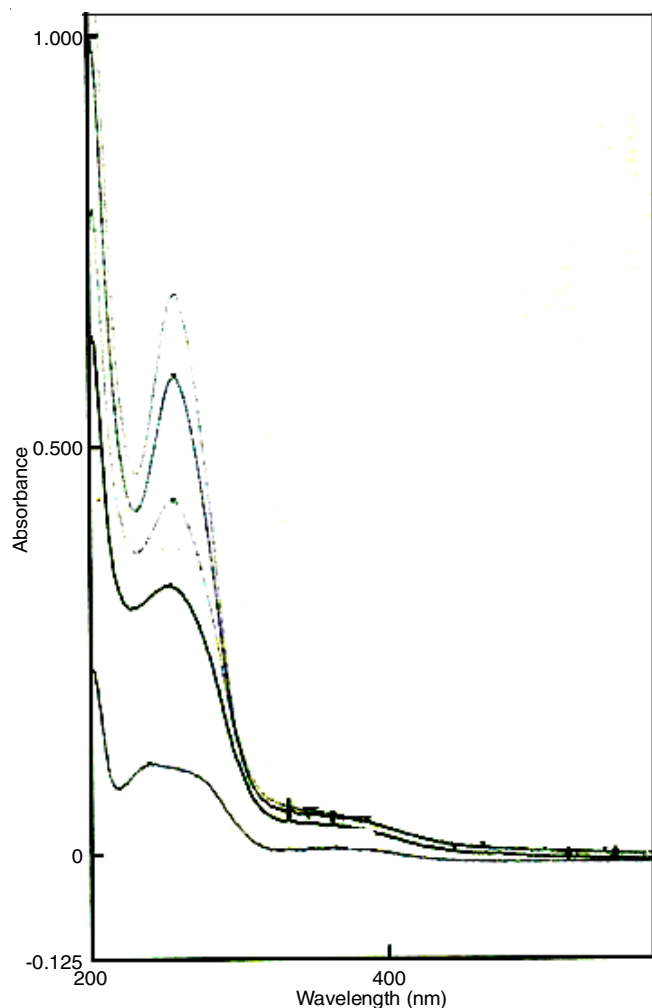


Fig. 9. Absorption spectra of chloro complexes of cobalt(II) in Tris-HCl buffer upon addition of different concentrations of CT-DNA

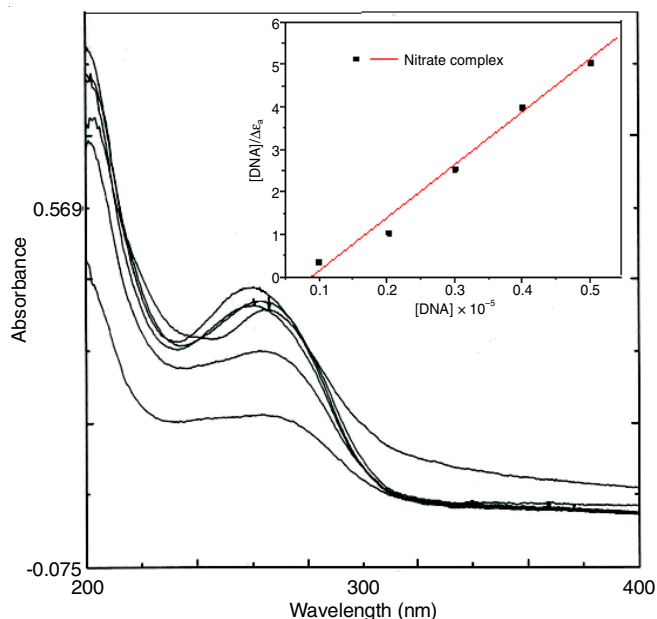


Fig. 8. Absorption spectra of nitrate complexes of cobalt(II) with increasing concentration of DNA. Plot of $[DNA]/\Delta\epsilon_a$ vs. $[DNA]$ for absorption titration of CT-DNA with complex

binder and nitrate complex shows a stronger binding ability towards DNA.

Fluorescence measurements: The fluorescence spectroscopy provides insight on the changes taken place in the microenvironment of DNA molecule on ligand binding. To further clarify the interaction of the complexes with DNA, the fluorescence spectral measurements were performed to determine the binding ability of the metal complexes with DNA. The binding of these compounds with CT-DNA were studied

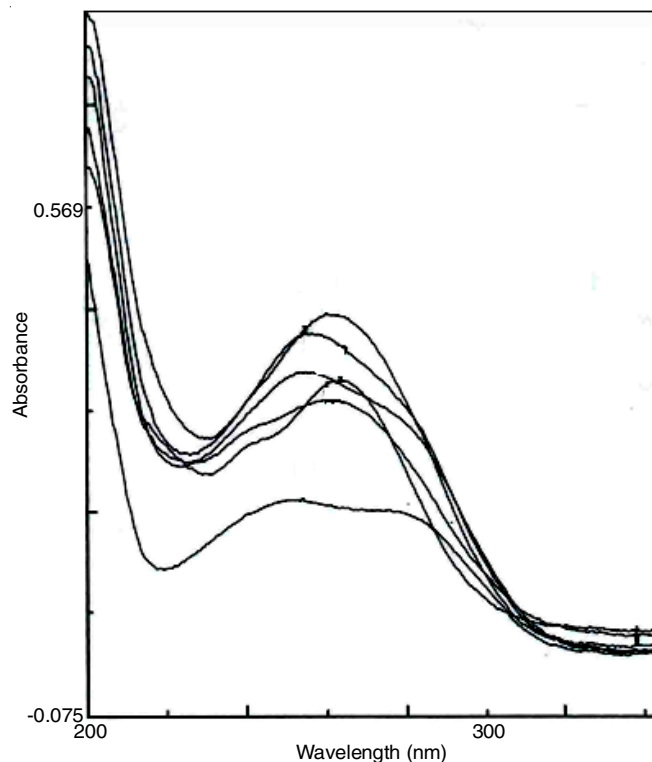


Fig. 10. Absorption spectra of bromo complexes of cobalt(II) in Tris-HCl buffer upon addition of different concentrations of CT-DNA

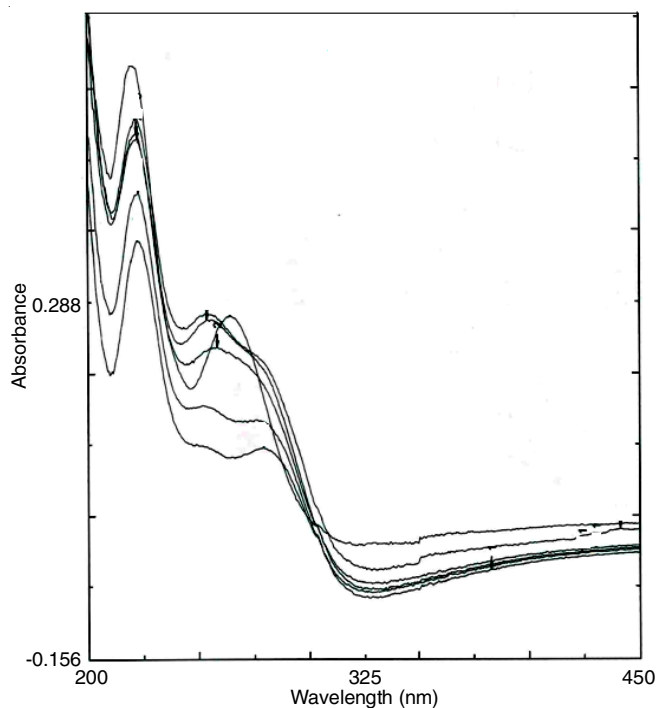


Fig. 11. Absorption spectra of iodide complexes of cobalt(II) in Tris-HCl buffer upon addition of different concentrations of CT-DNA

by monitoring the changes in the intrinsic fluorescence of these complexes at varying DNA concentration.

Figs. 12-14 show the fluorescence emission spectra of Co(II) complexes, $[\text{Co}(\text{BDAP})](\text{NO}_3)_2$ (**1**), $[\text{Co}(\text{BDAP})\text{Cl}_2]$ (**2**) and $[\text{Co}(\text{BDAP})\text{Br}_2]$ (**3**) upon excitation at 250 nm. Addition of DNA of different concentration to the complexes solution at constant concentration caused a gradual decrease in the fluorescence emission intensity. The spectra illustrate that an excess of DNA led to more effective quenching of the fluorophore molecule leads to fluorescence. The reduction of the emission intensity gives a measure of the DNA binding tendency of the complexes and stacking interaction (intercalation) between the adjacent DNA base pairs [49]. Fig. 15 illustrates that the quenching of complexes is in good agreement with the linear Stern-Volmer equation (eqn. 2) which provides further evidence that the complexes **1-3** bind to DNA [50]:

$$F_0/F = 1 + K_{sv}[Q] \quad (2)$$

where F_0 and F are the fluorescence intensities of complexes in the absence and presence of DNA (quencher), respectively, K_{sv} is the Stern-Volmer constant and $[Q]$ is the concentration of DNA. Plotting the relative emission intensities (F_0/F) against $[Q]$, the concentration of DNA for static process gives a linear Stern-Volmer plot which describes the static quenching process. The slope of this plotted line yields K_{sv} , the static quenching constant or associative equilibrium constant. The K_{sv} values for complexes **1-3** are $6.22 \times 10^3 \text{ M}^{-1}$ ($R = 0.9995$), $2.366 \times 10^3 \text{ M}^{-1}$ ($R = 0.9998$) and $2.254 \times 10^3 \text{ M}^{-1}$ ($R = 0.9993$), respectively. These results suggest that the interaction of complex **1** with ct-DNA is stronger than that of complex **2** and **3**, which is consistent with the above absorption spectral results. The quenching of the complexes fluorescence clearly indicated that the binding of the DNA to complexes molecules changed the microenvironment of fluorophore residue. The reduction in

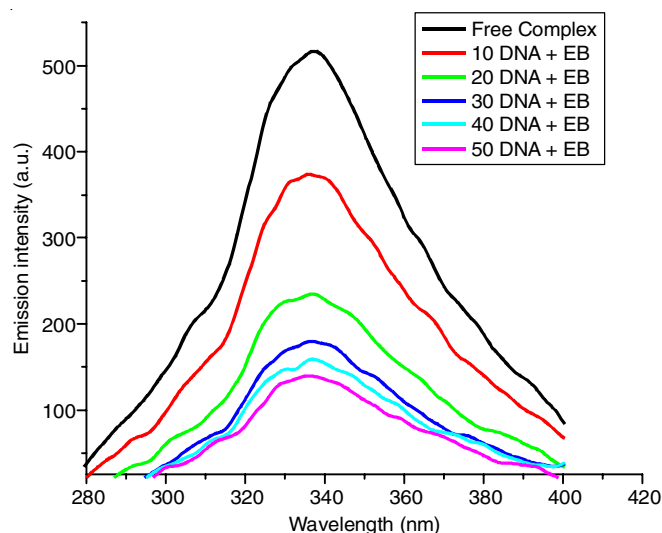


Fig. 12. Fluorescence emission spectra of $[\text{Co}(\text{BDAP})](\text{NO}_3)_2$

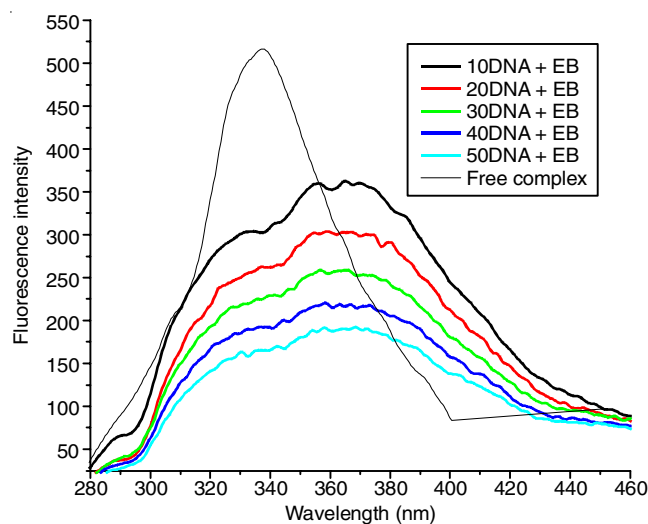


Fig. 13. Fluorescence emission spectra of $[\text{Co}(\text{BDAP})\text{Cl}_2]$ complexes

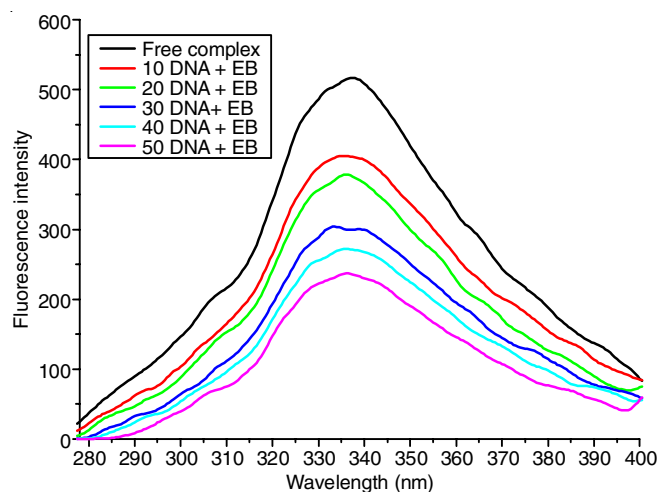


Fig. 14. Fluorescence emission spectra of $[\text{Co}(\text{BDAP})\text{Br}_2]$ complexes

the intrinsic fluorescence of these synthesized complex molecules upon interaction with DNA could be due to masking of compound fluorophore upon interaction between the stacked bases within the helix and/or surface binding at the reactive nucleophilic sites on the heterocyclic nitrogenous bases of DNA molecule [51].

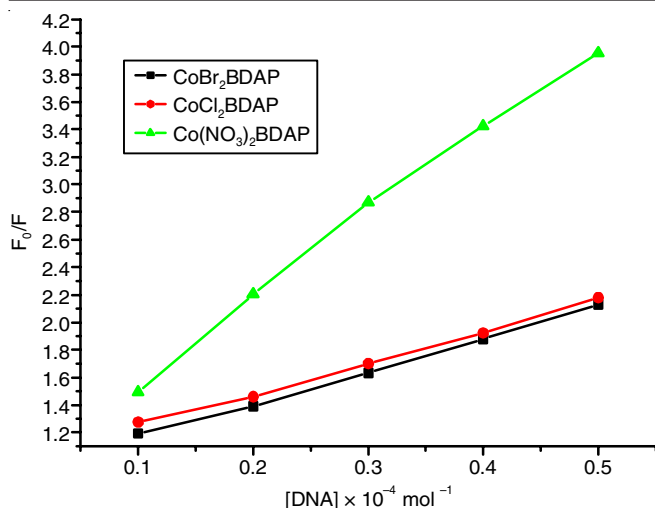


Fig. 15. Graphical representation of the ratio of F_0/F vs. DNA concentration of Co(II) complexes

Viscosity measurements: For further confirmation of the interactions between the complex and DNA, viscosity measurements were carried out. The viscosity and sedimentation measurements that are sensitive to length change are regarded as the most critical test of a binding in solution, in the absence of crystallographic structural data [52]. A classical intercalation model demands that the DNA helix must lengthen as base pairs are separated to accommodate the binding ligand, which leading to the increase of DNA viscosity. In contrast a partial and/or non-classical intercalation ligand could bend, then the DNA helix reduces its effective length concomitantly and its viscosity [53]. In the presence of complex, viscosity of DNA has been found to increase (Fig. 16). The increase in viscosity suggests that the complexes could bind to DNA by the intercalation binding mode.

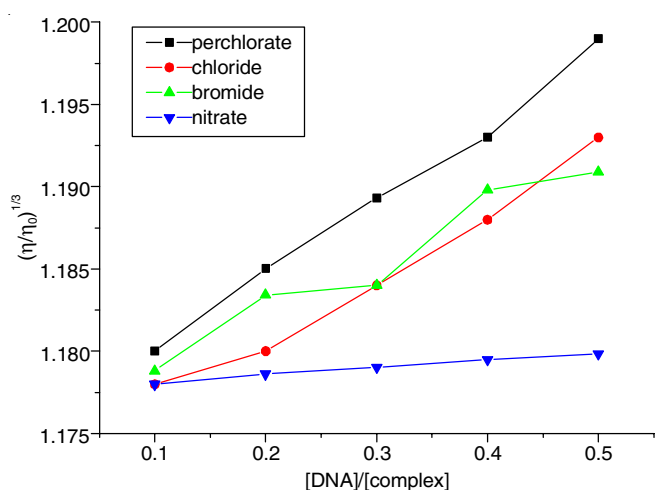


Fig. 16. Effect of increasing amounts of cobalt(II) complexes (1-4) on the relative viscosity of CT-DNA at 25 ± 0.01 °C

Conclusions

The elemental analyses and molar conductance data of the cobalt (II) complexes of BDAP indicate that the complexes may be formulated as $[\text{Co}(\text{BDAP})\text{X}_2]$ (where $\text{X} = \text{ClO}_4^-$, NO_3^- or I^-) and $[\text{Co}(\text{BDAP})\text{X}_2]$ (where $\text{X} = \text{Cl}^-$ or Br^-). The infrared spectral data suggest that BDAP acts as a neutral tetradentate

ligand coordinating through both the carbonyl oxygens and azomethine nitrogens. The molar conductance and the infrared spectral studies reveal that both the perchlorate, both the nitrate and both the iodide ions remain as counter ions and chloride and bromide ions are coordinated. The electronic spectra and magnetic moment suggest a octahedral geometry around the cobalt(II) ion in the chloro or bromo complexes and a tetrahedral geometry around the cobalt(II) ion in perchlorate, nitrate or iodide complexes. Molecular modeling of the proposed structure confirmed the octahedral and tetrahedral geometry for the respective molecules.

The thermal stability of the complexes were confirmed by thermogravimetric analyses. The mechanism for the thermal decomposition is random nucleation with one nucleus on each particle representing 'Mampel Model' for all the complexes in both the stages except the first stage thermal decomposition of chloride and perchlorate complexes. For the perchlorate complex, the mechanism is three dimensional diffusion spherical symmetry representing Ginstling- Brounshtien equation and for the chloride complex the mechanism is phase boundary reaction representing spherical symmetry. In antimicrobial studies all the complexes showed a good activity against the pathogenic bacteria and fungus than the ligand. From the DNA binding studies of the complexes it is concluded that the complexes showed a good affinity towards the DNA and binding is through intercalation. Based on the results of the present study, the tentative structures of the complexes are shown in Fig. 17.

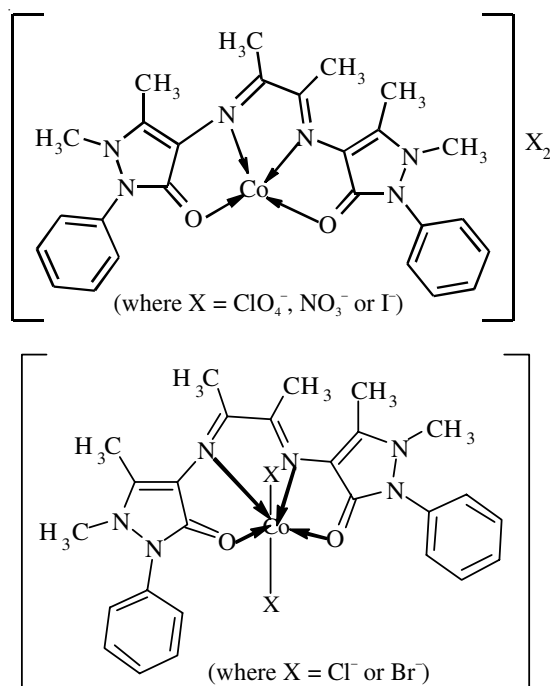


Fig. 17. Tentative structures of cobalt(II) complexes of BDAP

ACKNOWLEDGEMENTS

One of the authors (BNA) is thankful to University Grants Commission, New Delhi, India for providing RGNF fellowship. The authors are thankful to Mahatma Gandhi University, Kottayam, India for providing the laboratory facilities.

REFERENCES

- R.C. Maurya, A. Pandey, J. Chaurasia and H. Martin, *J. Mol. Struct.*, **798**, 89 (2006).
- M. Hasani and A. Rezaei, *Spectrochim. Acta*, **65A**, 1093 (2006).
- G. Turan-Zitouni, M. Sivaci, F.S. Kilic and K. Erol, *Eur. J. Med. Chem.*, **36**, 685 (2001).
- N.V. Bashkatova, E.I. Korotkova, Y.A. Karbainov, A.Y. Yagovkin and A.A. Bakibaev, *J. Pharm. Biomed. Anal.*, **37**, 1143 (2005).
- A.E. Rubtsov, R.R. Makhmudov, N.V. Kovylyayeva, N.I. Prosyaniuk, A.V. Bobrov and V.V. Zalesov, *Pharm. Chem. J.*, **36**, 608 (2002).
- D. Burdulene, A. Palaima, Z. Stumbryavichyute and Z. Talaikite, *Pharm. Chem. J.*, **33**, 191 (1999).
- A.N. Evstropov, V.E. Yavorovskaya, E.S. Vorob'ev, Z.P. Khudonogova, L.N. Gritsenko, E.V. Shmidt, S.G. Medvedeva, V.D. Filimonov, T.P. Prishchep and A.S. Saratikov, *Pharm. Chem. J.*, **26**, 426 (1992).
- G.H. Sayed, S.A. Shiba, A. Radwan, S.M. Mohamed and M. Khalil, *Chin. J. Chem.*, **10**, 475 (1992).
- J. Am. Coll. Toxicol.*, **11**, 475 (1992).
- M. Verleye, I. Heulard and J.-M. Gillardin, *Pharmacol. Res.*, **41**, 539 (2000).
- K. Saraswathi, N.V.S. Naidu, K.M. Kumari and K.P. Padmaja, *Chem. Environ. Res.*, **8**, 271 (1999).
- L. Singh, A. Sharma and S.K. Sindhu, *Asian J. Chem.*, **11**, 1445 (1999).
- Y. Zhang, Y. Li, H. Tao and L. Zhu, *Acta Crystallogr. Sect. E Struct. Rep. Online*, **58**, 24 (2002).
- A.I. Vogel, *A Text Book of Quantitative Inorganic Analysis*, ELBS, London (1961).
- E. Kurz, G. Kober and M. Berl, *Anal. Chem.*, **30**, 1958 (1983).
- O.N. Irobi, M. Moo-Young and W.A. Anderson, *Int. J. Pharm.*, **34**, 87 (1996).
- N. Raman, L. Mitu, A. Sakthivel and M.S.S. Pandi, *J. Iran. Chem. Soc.*, **6**, 738 (2009).
- Y.Z. Cai, Q. Luo, M. Sun and H. Corke, *Life Sci.*, **74**, 2157 (2004).
- K.E. Heim, A.R. Tagliaferro and D.J. Bobilya, *J. Nutr. Biochem.*, **13**, 572 (2002).
- G. Cohen and H. Eisenberg, *Biopolymers*, **8**, 45 (1969).
- W.J. Geary, *Coord. Chem. Rev.*, **7**, 81 (1971).
- S. Joseph and P.K. Radhakrishnan, *Synth. React. Inorg. Met.-Org. Chem.*, **28**, 423 (1998).
- M.T.H. Tarafder, N. Saravanan, K.A. Crouse and A.M. Ali, *Transition Met. Chem.*, **26**, 613 (2001).
- K.C. Raju, N.T. Madhu and P.K. Radhakrishnan, *Synth. React. Inorg. Met.-Org. Chem.*, **32**, 1115 (2002).
- K.P. Deepa and K.K. Aravindakshan, *Synth. React. Inorg. Met.-Org. Chem.*, **30**, 1601 (2000).
- M. Salehi, F. Rahimifar, M. Kubicki and A. Asadi, *Inorg. Chim. Acta*, **443**, 28 (2016).
- R.C. Maurya, D.D. Mishra, P.K. Trivedi and A. Gupta, *Synth. React. Inorg. Met.-Org. Nano-Met. Chem.*, **24**, 17 (1994).
- K. Das, T.N. Mandal, S. Roy, S. Gupta, A.K. Barik, P. Mitra, A.L. Rheingold and S.K. Kar, *Polyhedron*, **29**, 2892 (2010).
- N.T. Madhu and P.K. Radhakrishnan, *Synth. React. Inorg. Met.-Org. Nano-Met. Chem.*, **30**, 1561 (2000).
- K.Z. Ismail, *Transition Met. Chem.*, **25**, 522 (2000).
- P.M. Vimal Kumar and P.K. Radhakrishnan, *Polyhedron*, **29**, 2335 (2010).
- A.B.P. Lever, *Inorganic Electronic Spectroscopy*, Elsevier, Amsterdam, edn 2 (1984).
- M. del Carmen Fernández-Fernández, R.B. de la Calle, A. Macías, L.V. Matarranz and P. Pérez-Lourido, *Polyhedron*, **27**, 2301 (2008).
- A. Sousa-Pedrares, N. Camiña, J. Romero, M.L. Durán, J.A. García-Vázquez and A. Sousa, *Polyhedron*, **27**, 3391 (2008).
- M. Amirnasr, A.H. Mahmoudkhani, A. Gorji, S. Dehghanpour and H.R. Bijanzadeh, *Polyhedron*, **21**, 2733 (2002).
- S. Dehghanpour and A. Mahmoudi, *Synth. React. Inorg. Met.-Org. Nano-Met. Chem.*, **37**, 35 (2007).
- M. Tuncel and S. Serin, *Transition Met. Chem.*, **31**, 805 (2006).
- S. Mathew, C.G.R. Nair and K.N. Ninan, *Thermochim. Acta*, **144**, 33 (1989).
- M.E. Brown, *Introduction to Thermal Analysis-Techniques and Applications*, Chapman and Hall Ltd., New York (1988).
- M. Padmaja, J. Pragathi and C.G. Kumari, *J. Chem. Pharm. Res.*, **3**, 602 (2001).
- M. Tyagi, S. Chandra and P. Tyagi, *Spectrochim. Acta*, **117A**, 1 (2014).
- S. Chandra and A. Kumar, *Spectrochim. Acta*, **68A**, 1410 (2007).
- N. Raman and A. Selvan, *J. Mol. Struct.*, **985**, 173 (2011).
- M. Shebl, *Spectrochim. Acta*, **117A**, 127 (2014).
- F. Gao, H. Chao, F. Zhou, Y.-X. Yuan, B. Peng and L.N. Ji, *J. Inorg. Biochem.*, **100**, 1487 (2006).
- J.K. Barton, A.T. Danishefsky and J.M. Goldberg, *J. Am. Chem. Soc.*, **106**, 2172 (1984).
- V. Uma, M. Kanthimathi, T. Weyhermuller and B.U. Nair, *J. Inorg. Biochem.*, **99**, 2299 (2005).
- S. Anbu and M. Kandaswamy, *Polyhedron*, **30**, 123 (2011).
- N. Mudasar, N. Yoshioka and H. Inoue, *J. Inorg. Biochem.*, **77**, 239 (1999).
- S.O. Bahaffi, A.A. Abdel Aziz and M.M. El-Naggar, *J. Mol. Struct.*, **1020**, 188 (2012).
- M. Lee, A.L. Rhodes, M.D. Wyatt, S. Forrow and A. Hartley, *Biochemistry*, **32**, 4237 (1993).
- J.R. Lakowicz and G. Weber, *Biochemistry*, **12**, 4161 (1973).
- S. Satyanarayana, J.C. Dabrowiak and J.B. Chaires, *Biochemistry*, **31**, 9319 (1993).